

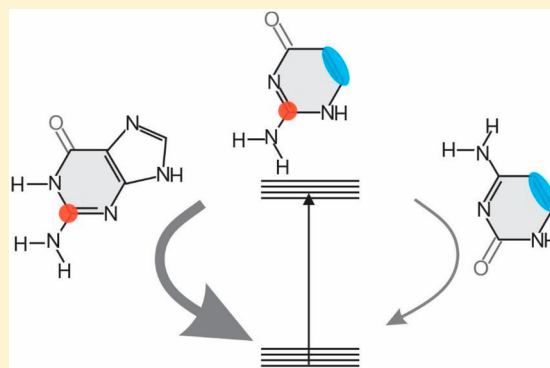
Excited-State Dynamics of Isocytosine: A Hybrid Case of Canonical Nucleobase Photodynamics

Jacob A. Berenbeim, Samuel Boldissar, Faady M. Siouri, Gregory Gate, Michael R. Haggmark, Briana Aboulache, Trevor Cohen, and Mattanjah S. de Vries*[✉]

Department of Chemistry and Biochemistry, University of California, Santa Barbara, California 93106-9510, United States

Supporting Information

ABSTRACT: We present resonant two-photon ionization (R2PI) spectra of isocytosine (isoC) and pump–probe results on two of its tautomers. IsoC is one of a handful of alternative bases that have been proposed in scenarios of prebiotic chemistry. It is structurally similar to both cytosine (C) and guanine (G). We compare the excited-state dynamics with the Watson–Crick (WC) C and G tautomeric forms. These results suggest that the excited-state dynamics of WC form of G may primarily depend on the heterocyclic substructure of the pyrimidine moiety, which is chemically identical to isoC. For WC isoC we find a single excited-state decay with a rate of $\sim 10^{10} \text{ s}^{-1}$, while the enol form has multiple decay rates, the fastest of which is 7 times slower than for WC isoC. The excited-state dynamics of isoC exhibits striking similarities with that of G, more so than with the photodynamics of C.



Without a fossil record of the prebiotic chemical world we are left to conjecture to understand the roadmap that led to RNA and DNA. One of the factors that may have played a role in the prebiotic chemistry on an early earth is the photochemistry that could have been important before modern enzymatic repair and before the formation of the ozone layer.^{1–6} Nucleobases, when absorbing ultraviolet (UV) radiation, tend to eliminate the resulting electronic excitation by internal conversion (IC) in picoseconds (ps) or less.^{4,7–9} The availability of this rapid “safe” de-excitation pathway turns out to depend exquisitely on molecular structure. DNA and RNA bases are generally short-lived in the excited state, and thus UV-protected, while many closely related compounds are long-lived and thus more prone to UV damage. This structure dependence suggests a mechanism for the chemical selection of the building blocks of life, implying that photochemical properties may be molecular fossils of the earliest stages of prebiotic chemistry.

It is therefore of great interest to study the photochemical properties of possible alternative bases in comparison to the canonical bases. Especially intriguing are structures that can form alternate base pairs with the same Watson–Crick (WC) motif as the canonical ones, such as the triple hydrogen bonded guanine/cytosine (G/C) pair.^{10–13} The alternative bases isocytosine (isoC) and isoguanine (isoG) were predicted in 1962 as a plausible third WC base pair.¹⁴ As pointed out by Saladino et al., isoC can form WC base pairs with cytosine (C) and isoguanine or a reversed WC base pair with guanine.¹⁵ Here we focus on isoC, which is not only an isomer of C but also an analogue of guanine (G), see Figure 1. Theoretical and

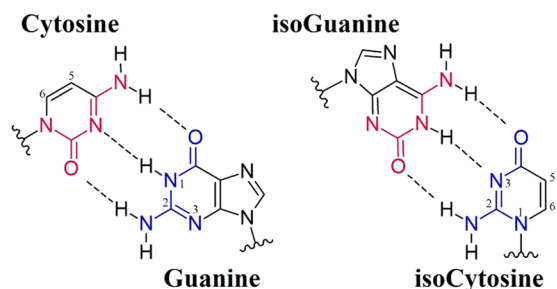


Figure 1. Structures of G/C and isoG/isoC arranged to emphasize heterocyclic substructure similarities, emphasized in red and blue.

experimental study has established the thermodynamic stability of the isoC/isoG base pair which nominally has greater free energy than G/C as well as of other possible base pair combinations with isoC.^{16,17} This has piqued interest in the prebiotic prevalence of these unnatural pairs in addition to their role in synthetic research and medical applications.^{18,19} Here we aim to understand the photostability of isoC.

We have arranged the bases within Figure 1 to emphasize the functional rearrangement from the standard base to its iso-analog about the pyrimidine heterocyclic centers. Doing so likens isoC to the core moiety of G. The difference between G and isoC is the five-membered ring in G (not present in isoC) which would have consequences for formation of a macro-

Received: August 3, 2017

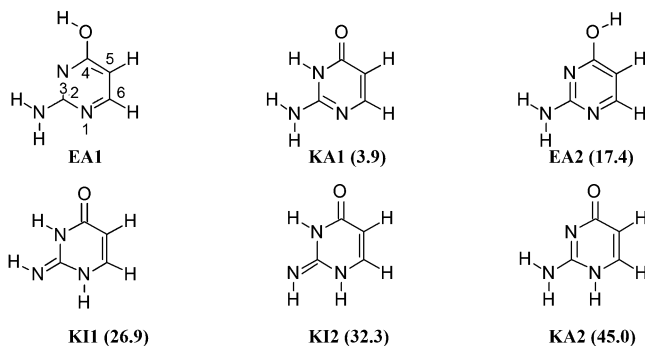
Accepted: October 6, 2017

Published: October 6, 2017

molecular structure. In this work, we find that the excited-state dynamics of isoC exhibits striking similarities with that of G and more so than with the photodynamics of C.

IsoC has previously been identified in the gas phase,²⁰ and its photo dynamics have been studied theoretically^{21,22} and in the condensed phase.^{23–25} However, no excited-state lifetime has been experimentally determined of isolated isoC in individual tautomeric forms. The two lowest-energy forms are enol and keto which can isomerize via an excited-state intramolecular proton transfer. This isomerization after UV excitation has been observed in solution²³ by time-dependent absorption spectroscopy and in a rare gas matrix by changes in the IR absorption.^{24,25} Chart 1 outlines the lowest-energy tautomers

Chart 1. Lowest Ground-State Energy Structures ($\Delta E < 50$ kJ/mol)^a



^aHeterocyclic atoms are numbered for EA1, but the convention is the same for all others. Arranged in order of relative energy given in parentheses (kJ/mol). Zero-point corrected energies were calculated by DFT analysis with the B3LYP hybrid functional and with a cc-pVTZ basis set.

in the gas phase. KA2 corresponds to the WC structure in the pairing with isoG in Figure 1. KA1 can also form similar triple hydrogen bonded structures with other tautomeric forms of G, such as the enol form.

Recent work by Szabla et. al used state-of-the-art surface-hopping adiabatic molecular dynamic simulations to predict the excited-state lifetime of isoC to be the following: $\tau_{EA1} = 533$ fs and $\tau_{KA1} = 182$ fs.²¹ These lifetimes are from populating a continuum of mixed character electronic states S1–S6 at the 5.5 ± 0.2 eV spectral domain which proceed to relax through S1 IC. Three dominant conical intersection (CI) geometries are established in their work for the modeled EA1 and KA1 starting structures, whereby pyramidalization of the planar Franck–Condon (FC), i.e. excitation geometry, structure at the C2 position accounts for $\Phi_{EA1} = 0.60$ and $\Phi_{KA1} = 0.93$ nonradiative relaxation yields, while deformation about the C₅=C₆ bond accounts for a CI of negligible yield. Hu et al. also studied the KA1 form computationally, comparing different levels of theory. They assumed excitation at energies closer to the vibrationless level and identified three CIs, all leading to IC to the ground state, one involving the C=O stretching vibration and two involving out-of-plane structures of the NH₂ group. They found the preferred pathway to depend on the computational method, as did the IC rate, leading to excited-state lifetimes ranging from 100 fs to 1 ps.²⁶ Surprisingly, both computational studies are contrary to the bulk of theoretical work done on pyrimidine relaxation dynamics, where the CI_{C₅=C₆} is understood to be a major

pathway toward nonradiative deactivation by twisting of the H–C₅=C₆–H torsional angle to near ethylene geometry.^{27–29}

Trachsel et al. most recently showed the importance of this particular bond deformation when they measured excited-state lifetimes of 5,6-trimethylenecytosine, a sterically constrained C analogue, in the gas phase.³⁰ This modified version yielded lifetimes attributed to IC six times greater than that of C, likely due to the absence of a CI_{C₅=C₆}.

Figure 2 shows two-color (2C) resonant two-photon ionization (R2PI) spectra of isocytosine with nanosecond

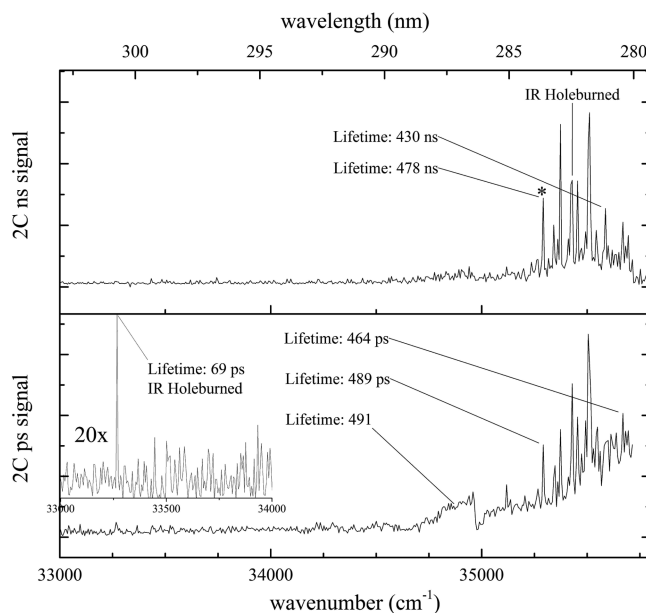


Figure 2. 2C R2PI spectra for isocytosine (a) ns excitation with 193 nm ionization and (b) ps excitation with 213 nm ionization (5th Nd:YAG harmonic). Lifetimes are pump–probe data. See text for details.

(ns) and ps pulse sources. The ns spectrum (Figure 2a) has a well-defined origin transition at 35292 cm^{-1} (starred *) followed by a series of discrete peaks atop an elevated baseline over a range of 500 cm^{-1} . This elevated baseline extends to the red but is relatively low in intensity and devoid of features. The ps trace (Figure 2b) exhibits the same defined vibronic transitions seen in the ns spectrum but presents another unique feature at 33266 cm^{-1} . Here, the elevated baseline features to the red of the starred origin are by contrast to the ns spectrum more intense. While this signal could result from other tautomers, we suspect that this feature is due to hot bands from the low-frequency breathing vibrational modes which are more efficiently excited with the 6 cm^{-1} spectral line width of ps laser and artificially intensified by elevated laser power in that region. The sharp feature at 35000 cm^{-1} is a laser power artifact and highlights the nonresonant nature of the absorption in this range. Furthermore, we could not obtain an IR–UV double-resonant signal from this part of the spectrum, which is also consistent with hot bands. We simultaneously recorded wavelength and mass spectra, shown as a two-dimensional plot in the Supporting Information (Figure S.1) to verify that there is no contribution to the isoC mass channel from potential higher-order clusters, including checking the M+1 mass channel.

IR–UV double-resonance spectroscopy reveals the presence of the EA1 tautomer, with the origin at 35292 cm^{-1} and the

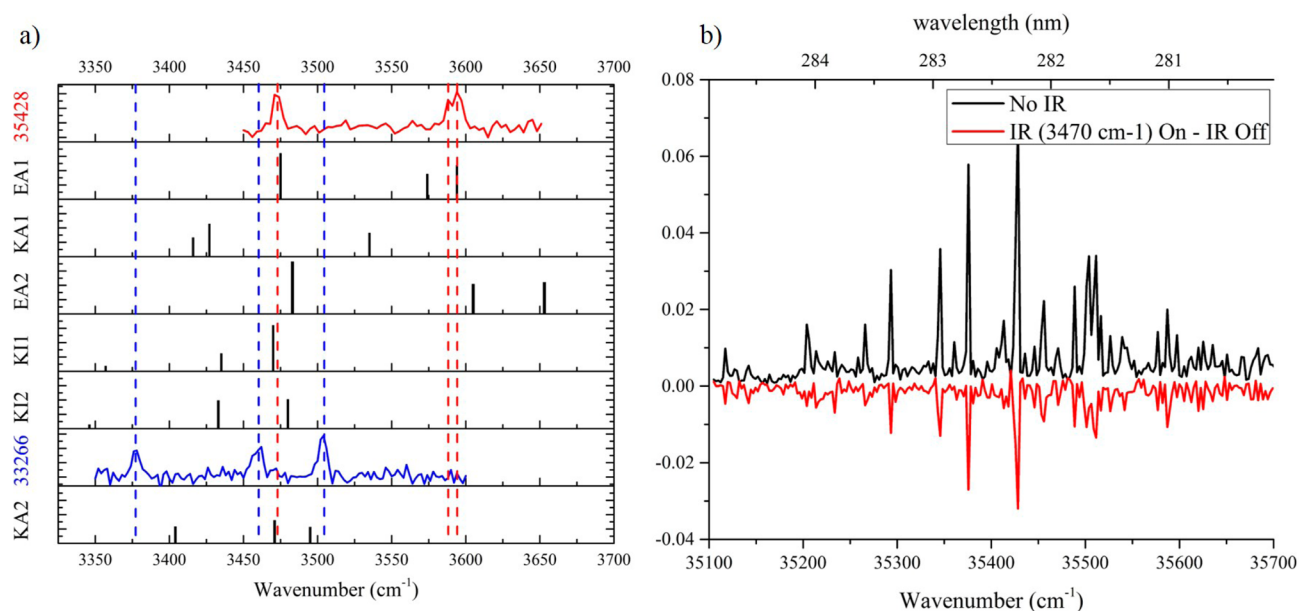


Figure 3. (a) IR UV hole burning results compared to anharmonic simulations for the six low-energy structures. Experimental spectra are from UV ns probe 35 428 (red) and ps probe 33 266 (blue) cm^{-1} , respectively. (b) Nanosecond 2C R2PI spectrum (black) and the difference trace below (red) when burning at the EA1 experimental wavelength of 3 470 cm^{-1} . Anharmonic DFT analysis calculated with the B3LYP hybrid functional and the cc-pVTZ basis set.

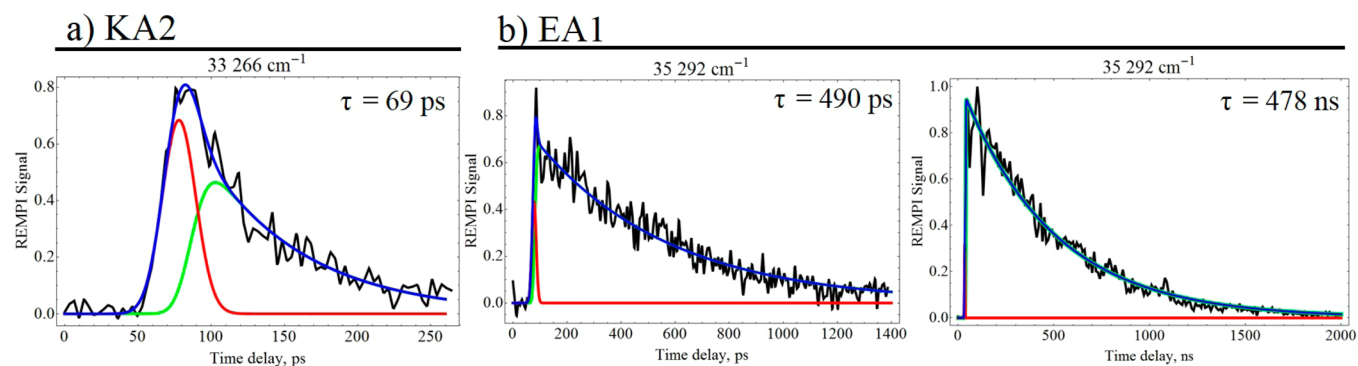


Figure 4. Pump-probe results from the origin bands of (a) the KA2 and (b) the EA1 tautomer in the ps and ns regimes. The data in panels a and b are fit to a curve (blue) which is the sum of a single exponential decay convolved with a Gaussian component (green) representative of our instrument response function (IRF) and the IRF itself (red).

KA2 tautomer, with the feature at 33 266 cm^{-1} , shown by Figure 3a. We matched IR-UV hole burning spectra (probed as annotated in Figure 3a) with anharmonic computations. The peaks observed in the ns 2C R2PI scan are all correlated with the EA1 tautomer by IR-UV double-resonance spectroscopy in which the IR resonance at 3 470 cm^{-1} was held constant 200 ns prior to scanning the UV source (Figure 3b). We have attached UV-UV hole burning results at 35 428 cm^{-1} as Figure S.2 which further confirms that all the peaks shown in the ns spectrum belong to a single tautomer which we identify as EA1. After characterization, the KA2 and EA1 electronic origin transition energies correlated to within 10% of those predicted for KA1 and EA1 by Szabla et al. and KA1 by Hu et al.^{21,26}

Referring to Chart 1, KA2 is predicted to be the highest-energy structure indicating that if this tautomer is present all other forms may be present in our beam as well. Jet-cooling is not an equilibrium process; therefore, we cannot predict the tautomer distribution, but in our experience in our setup usually the lowest-energy tautomers up to typically about 50 kJ/mol are present. Furthermore, the KA1 tautomer was

observed in matrix isolation experiments.^{24,25} Three possible reasons certain tautomers are not observed in our experiment are the following. (1) There can be tautomers that absorb in different ranges of the UV spectrum, which we have not covered. (2) Our experiment measures action spectroscopy rather than direct absorption. It is possible that a molecule is excited by the first photon but not ionized by the second. One way this situation can occur is when the excited-state lifetime is significantly shorter than the ionizing laser pulse. A very similar situation exists for guanine: the lowest-energy keto tautomers, equivalent to KA1 in isoC, have not been observed so far by R2PI, although from direct absorption in microwave experiments and in He droplets they are known to exist.^{31,32} (3) A molecule may undergo fragmentation after excitation or ionization adding complexity to the action spectrum as we typically monitor only the parent ion mass. We did not observe any obvious nonstatistical fragmentation.

Figure 4 shows a selection of the pump-probe results from the origin transitions of EA1 and KA2; additional pump-probe fits are found in Figure S.3. The derived lifetimes are shown

within Figure 2a,b. The 463–491 ps lifetime of the EA1 tautomer represents the decay rate of the excited state. All pump–probe curves were fit to a monoexponential decay.

We probed the broad elevated baseline signal present to the red of the EA1 origin in Figure 2a in hopes of attributing it to a specific species from Chart 1. The lifetime of 491 ps agrees with the ps component measured for EA1. We were unable to support this pump–probe correlation to EA1 with conclusive IR–UV hole burning results, like those from Figure 3a. The inability to obtain a clear IR–UV spectrum would be consistent with hot bands.

Table 1 lists vibrationless excited-state lifetimes, following 0–0 excitation unless otherwise noted, which we found here for

Table 1. Vibrationless Excited-State Lifetimes^a

	keto KA1	keto KA2	enol
isocytosine	N/O	69 ps	489 ps/478 ns
cytosine	N/O	730 ps ³³ /290 ns ³⁴	56 ps ^b /30.5 ns ^b
guanine	N/O	N/O	13 ns ³⁵ /40 ns ³⁵

^aN/O = not observed. ^bThese reported pump–probe results for enol-C were not obtained at the 0–0 transition but rather on the rising edge of its broad initial absorption region.

isoC and compares those with the equivalent lifetimes for C and G. In terms of its photodynamics, isoC has elements of both G and C. The six-membered ring in G is an amino-pyrimidione, identical to isoC with a five-membered ring that immobilizes the C5=C6 bond that is free in isoC. Szabla et al. identified major conical intersections involving ring puckering, C=O stretching, NH₂ out-of-plane bending, and C=C rotation.²¹ The former three are similar to the CIs that dominate G dynamics,³⁶ while the latter cannot occur in G but is characteristic for pyrimidines, including cytosine.³⁷

We first compare isoC with G. Neither the 1H-9h-keto-amino (KA1 equiv) nor the 3H-keto-amino (KA2 equiv) have been identified yet by ps or ns R2PI. So in both isoC and G we do not observe the KA1 form (because of the difference in numbering between pyrimidines and purines, this is N3H for isoC and N1H for G, see Figure 1). For G this is the WC form and is slightly less in energy than the imino forms, which are observed.^{36,38} As noted before, one likely reason for not observing a species with R2PI is an excited-state lifetime significantly shorter than the laser pulse length. In the G experiments pulse widths were of the order of 5 ns, and in the current isoC experiments they are lower limited at 30 ps. Excited states with lifetimes of the order of a few hundred femtoseconds could thus defy detection by R2PI in these experiments. Notably, the conical intersection that is most responsible for the ultrafast IC in the G keto case involves pyramidalization at the C2 position and does not involve the 5-membered ring.^{29,36,39,40} Therefore, it is possible for the isoC KA1 form to undergo very similar ultrafast IC. For the KA2 form of isoC we find a lifetime of 69 ps, while the equivalent form for G was not observed with R2PI although it is lower in energy than the imino forms that are observed with R2PI.^{31,32,41} For both compounds the enol form is significantly longer-lived, with two independent decay channels of almost 0.5 ns and 0.5 μ s for isoC and 13 and 40 ns for G.³⁵ In both cases we consider that the long-lived dark state could be a triplet state and for G the 13 ns decay can be attributed to fluorescence.⁴² In the case of enol isoC the observation of two decays with a 3 orders of magnitude difference implies that

those two channels do not decay from the same excited state. If they did, the higher rate process would have 3 orders of magnitude larger quantum yield and dwarf the signal from the lower rate process. Instead we assume an ultrafast population of a doorway state, possibly a triplet, which in turn decays at the slow rate.

In comparing isoC and C, we notice larger differences in excited-state dynamics. Again we do not see the KA1 equivalent form for C, which is about 30 kJ/mol higher in energy than the WC KA2 equivalent and enol forms. The KA2 form, which is the lowest-energy keto form for C, behaves very different from isoC. Leutwyler and co-workers have reported this case in great detail, finding a vibrationless decay time of 730 ps.^{33,43–45} Nir et al. reported on a long-lived state, presumably a triplet, with a 290 ns lifetime.^{34,46} These observations suggest different dynamics than for isoC where we found a single 69 ps decay. For the enol form of C we find a 56 ps short component which populates a longer-lived state with a 30.5 ns lifetime (shown in Figure S.4). Because the ns R2PI spectra of enol C, also reported by Nir et al., is broad and without a clear 0–0 transition,⁴⁶ we performed these pump–probe measurements on the rising edge of the broad signal which appears along with the ps 2C R2PI in Figure S.4. So for C the vibrationless excited state for the enol form is shorter lived than for the keto form, contrary to the situation for both G and isoC. Szabla et al. find a CI for the isoC enol that involves the C5=C6 twist, which also plays a role in C; however, according their calculations, only 14% of the trajectories follow this path in isoC.²¹ It should be noted that their trajectories start at 5.5 ± 0.2 eV, which is a full electronvolt more excited-state energy than what we impart in our experiments. This may suggest that the C5=C6 CI for EA1 has an energy barrier of up to 1 eV.

The conclusion that isoC resembles G in its photochemistry is just one of the considerations in evaluating its potential role in prebiotic scenarios. For example, we are currently investigating the photostability of isoguanine as one of its possible alternative base pair partners. Furthermore, the response to radiation is wavelength-dependent, and its consideration should not be limited to a single wavelength or small parts of the spectrum. The study of the dynamics near the threshold for absorption provides opportunities to probe the potential energy landscape close to the most relevant CIs and barriers. It is hoped that these data will serve as support for further detailed theoretical treatments.

EXPERIMENTAL SECTION

Here we report results which identify the EA1 and KA2 tautomers of cold isocytosine prepared in a molecular beam. We have investigated the absorption spectrum with 2C R2PI, identified the tautomers with IR–UV hole burning, and performed pump–probe experiments to probe excited-state relaxation dynamics in the ns and ps time regimes. The instrument and explanation of these specific techniques are detailed elsewhere and very briefly outlined here.^{35,47} IsoC standard (Sigma, $\geq 99\%$) is entrained into a pulsed molecular beam by laser desorption and ionized by tunable 2C R2PI. The ps spectroscopic and pump–probe delay measurements are performed with a Nd:YAG driven optical parametric oscillator (OPG) laser system which produces ~ 30 ps laser pulses. The molecule is excited by the tunable light from the OPG and ionized by 213 nm, which is mechanically delayed up to 1.5 ns before colineation with the OPG beam. A variable electronic delay between the OPG UV laser and an excimer laser (193

nm, 6 ns pulse width) is used for spectroscopic and pump–probe measurements in the ns time delay range.

For IR–UV double-resonant spectroscopy, an optical parametric oscillator/amplifier (OPO/OPA) precedes the 2C R2PI by 200 ns. IR resonant frequencies are compared to anharmonic DFT analysis calculated with the B3LYP hybrid functional with the cc-pVTZ basis set.

■ ASSOCIATED CONTENT

Supporting Information

The Supporting Information is available free of charge on the ACS Publications website at DOI: [10.1021/acs.jpcllett.7b02032](https://doi.org/10.1021/acs.jpcllett.7b02032).

Two-dimensional TOF data, double-resonant UV–UV spectrum of EA1 isoC, and additional pump–probe results of EA1 isoC and enol C (PDF)

■ AUTHOR INFORMATION

Corresponding Author

*E-mail: devries@chem.ucsb.edu.

ORCID

Mattanjah S. de Vries: 0000-0001-5007-8074

Notes

The authors declare no competing financial interest.

■ ACKNOWLEDGMENTS

This work was supported by National Aeronautics and Space Administration Grant NNX12AG77G and by the National Science Foundation under CHE-1301305. We acknowledge support from the Center for Scientific Computing from the CNSI, MRL: an NSF MRSEC (DMR-1121053), and NSF CNS-0960316.

■ REFERENCES

- (1) Beckstead, A. A.; Zhang, Y. Y.; De Vries, M. S.; Kohler, B. Life in the Light: Nucleic Acid Photoproperties as a Legacy of Chemical Evolution. *Phys. Chem. Chem. Phys.* **2016**, *18*, 24228–24238.
- (2) Nir, E.; Kleinermanns, K.; Grace, L.; De Vries, M. S. On the Photochemistry of Purine Nucleobases. *J. Phys. Chem. A* **2001**, *105*, 5106–5110.
- (3) Rios, A. C.; Tor, Y. On the Origin of the Canonical Nucleobases: An Assessment of Selection Pressures across Chemical and Early Biological Evolution. *Isr. J. Chem.* **2013**, *53*, 469–483.
- (4) Middleton, C. T.; De La Harpe, K.; Su, C.; Law, Y. K.; Crespo-Hernandez, C. E.; Kohler, B. DNA Excited-State Dynamics: From Single Bases to the Double Helix. *Annu. Rev. Phys. Chem.* **2009**, *60*, 217–239.
- (5) Miller, S. L.; Orgel, L. E. *The Origins of Life on the Earth*; Prentice-Hall: Englewood Cliffs, NJ, 1974.
- (6) Gustavsson, T.; Improta, R.; Markovitsi, D. DNA/Rna: Building Blocks of Life under Uv Irradiation. *J. Phys. Chem. Lett.* **2010**, *1*, 2025–2030.
- (7) Kohler, B. Nonradiative Decay Mechanisms in DNA Model Systems. *J. Phys. Chem. Lett.* **2010**, *1*, 2047–2053.
- (8) Kleinermanns, K.; Nachtigallová, D.; De Vries, M. S. Excited State Dynamics of DNA Bases. *Int. Rev. Phys. Chem.* **2013**, *32*, 308–342.
- (9) Crespo-Hernandez, C. E.; Martinez-Fernandez, L.; Rauer, C.; Reichardt, C.; Mai, S.; Pllum, M.; Marquetand, P.; Gonzalez, L.; Corral, I. Electronic and Structural Elements That Regulate the Excited-State Dynamics in Purine Nucleobase Derivatives. *J. Am. Chem. Soc.* **2015**, *137*, 4368–4381.
- (10) Yang, Z. Y.; Hutter, D.; Sheng, P. P.; Sismour, A. M.; Benner, S. A. Artificially Expanded Genetic Information System: A New Base Pair

with an Alternative Hydrogen Bonding Pattern. *Nucleic Acids Res.* **2006**, *34*, 6095–6101.

(11) Leontis, N. B.; Stombaugh, J.; Westhof, E. The Non-Watson-Crick Base Pairs and Their Associated Isostericity Matrices. *Nucleic Acids Res.* **2002**, *30*, 3497–3531.

(12) Wojciechowski, F.; Leumann, C. J. Alternative DNA Base-Pairs: From Efforts to Expand the Genetic Code to Potential Material Applications. *Chem. Soc. Rev.* **2011**, *40*, S669–S679.

(13) Cafferty, B. J.; Hud, N. V. Was a Pyrimidine-Pyrimidine Base Pair the Ancestor of Watson-Crick Base Pairs? Insights from a Systematic Approach to the Origin of Rna. *Isr. J. Chem.* **2015**, *55*, 891–905.

(14) Rich, A. On the Problems of Evolution and Biochemical Information Transfer. In *Horizons in Biochemistry*; Kasha, M., Pullman, B., Ed; Academic Press: New York, 1962; pp 103–126.

(15) Saladino, R.; Crestini, C.; Cossetti, C.; Di Mauro, E.; Deamer, D. Catalytic Effects of Murchison Material: Prebiotic Synthesis and Degradation of Rna Precursors. *Origins Life Evol. Biospheres* **2011**, *41*, 437–451.

(16) Roberts, C.; Bandaru, R.; Switzer, C. Theoretical and Experimental Study of Isoguanine and Isocytosine: Base Pairing in an Expanded Genetic System. *J. Am. Chem. Soc.* **1997**, *119*, 4640–4649.

(17) Yang, X. L.; Sugiyama, H.; Ikeda, S.; Saito, I.; Wang, A. H. Structural Studies of a Stable Parallel-Stranded DNA Duplex Incorporating Isoguanine:Cytosine and Isocytosine:Guanine Basepairs by Nuclear Magnetic Resonance Spectroscopy. *Biophys. J.* **1998**, *75*, 1163–1171.

(18) Sismour, A. M.; Benner, S. A. The Use of Thymidine Analogs to Improve the Replication of an Extra DNA Base Pair: A Synthetic Biological System. *Nucleic Acids Res.* **2005**, *33*, 5640–5646.

(19) Hirao, I. Unnatural Base Pair Systems for DNA/Rna-Based Biotechnology. *Curr. Opin. Chem. Biol.* **2006**, *10*, 622–627.

(20) Lee, S. J.; Min, A.; Ahn, A.; Moon, C. J.; Choi, M. Y.; Ishiuchi, S.-I.; Miyazaki, M.; Fujii, M. Resonance Enhanced Multi-Photon Ionization (Rempi) and Double Resonance (UV-UV and IR-UV) Spectroscopic Investigation Isocytosine. International Symposium on Molecular Spectroscopy, June 17–21, 2013; Ohio State University: Columbus, OH.

(21) Szabla, R.; Gora, R. W.; Sponer, J. Ultrafast Excited-State Dynamics of Isocytosine. *Phys. Chem. Chem. Phys.* **2016**, *18*, 20208–20218.

(22) Shukla, M. K.; Leszczynski, J. Investigations of the Excited-State Properties of Isocytosine: An Ab Initio Approach. *Int. J. Quantum Chem.* **2000**, *77*, 240–254.

(23) Bakalska, R. I.; Delchev, V. B. Comparative Study of the Relaxation Mechanisms of the Excited States of Cytosine and Isocytosine. *J. Mol. Model.* **2012**, *18*, 5133–5146.

(24) Ivanov, A. Y.; Stepanian, S. G.; Adamowicz, L. Tautomeric Transitions of Isocytosine Isolated in Argon and Neon Matrices Induced by Uv Irradiation. *J. Mol. Struct.* **2012**, *1025*, 92–104.

(25) Vranken, H.; Smets, J.; Maes, G.; Lapinski, L.; Nowak, M. J.; Adamowicz, L. Infrared Spectra and Tautomerism of Isocytosine; an Ab Initio and Matrix Isolation Study. *Spectrochimica Acta Part A: Molecular Spectroscopy* **1994**, *50*, 875–889.

(26) Hu, D.; Liu, Y. F.; Sobolewski, A. L.; Lan, Z. Nonadiabatic Dynamics Simulation of Keto Isocytosine: A Comparison of Dynamical Performance of Different Electronic-Structure Methods. *Phys. Chem. Chem. Phys.* **2017**, *19*, 19168–19177.

(27) Merchan, M.; Gonzalez-Luque, R.; Climent, T.; Serrano-Andres, L.; Rodriguez, E.; Reguero, M.; Peláez, D. Unified Model for the Ultrafast Decay of Pyrimidine Nucleobases. *J. Phys. Chem. B* **2006**, *110*, 26471–26476.

(28) Pepino, A. J.; Segarra-Martí, J.; Nenov, A.; Improta, R.; Garavelli, M. Resolving Ultrafast Photoinduced Deactivations in Water-Solvated Pyrimidine Nucleosides. *J. Phys. Chem. Lett.* **2017**, *8*, 1777–1783.

(29) Improta, R.; Santoro, F.; Blancafort, L. Quantum Mechanical Studies on the Photophysics and the Photochemistry of Nucleic Acids and Nucleobases. *Chem. Rev.* **2016**, *116*, 3540–3593.

(30) Trachsel, M. A.; Lobsiger, S.; Schär, T.; Blancafort, L.; Leutwyler, S. Planarizing Cytosine: The S1 State Structure, Vibrations, and Nonradiative Dynamics of Jet-Cooled 5,6-Trimethylenecytosine. *J. Chem. Phys.* **2017**, *146*, 244308.

(31) Choi, M. Y.; Miller, R. E. Four Tautomers of Isolated Guanine from Infrared Laser Spectroscopy in Helium Nanodroplets. *J. Am. Chem. Soc.* **2006**, *128*, 7320–7328.

(32) Mons, M.; Piuze, F.; Dimicoli, I.; Gorb, L.; Leszczynski, J. Near-Uv Resonant Two-Photon Ionization Spectroscopy of Gas Phase Guanine: Evidence for the Observation of Three Rare Tautomers. *J. Phys. Chem. A* **2006**, *110*, 10921–10924.

(33) Blaser, S.; Trachsel, M. A.; Lobsiger, S.; Wiedmer, T.; Frey, H. M.; Leutwyler, S. Gas-Phase Cytosine and Cytosine-N1-Derivatives Have 0.1–1 Ns Lifetimes near the S1 State Minimum. *J. Phys. Chem. Lett.* **2016**, *7*, 752–757.

(34) Nir, E.; Muller, M.; Grace, L. I.; De Vries, M. S. Rempy Spectroscopy of Cytosine. *Chem. Phys. Lett.* **2002**, *355*, 59–64.

(35) Siouri, F. M.; Boldissar, S.; Berenbeim, J. A.; De Vries, M. S. Excited State Dynamics of 6-Thioguanine. *J. Phys. Chem. A* **2017**, *121*, 5257–5266.

(36) Marian, C. M. The Guanine Tautomer Puzzle: Quantum Chemical Investigation of Ground and Excited States. *J. Phys. Chem. A* **2007**, *111*, 1545–1553.

(37) Kistler, K. A.; Matsika, S. Radiationless Decay Mechanism of Cytosine: An Ab Initio Study with Comparisons to the Fluorescent Analogue 5-Methyl-2-Pyrimidinone. *J. Phys. Chem. A* **2007**, *111*, 2650–2661.

(38) Mons, M.; Dimicoli, I.; Piuze, F. Isolated Guanine: Tautomerism, Spectroscopy and Excited State Dynamics. In *Radiation Induced Molecular Phenomena in Nucleic Acids: A Comprehensive Theoretical and Experimental Analysis*; Shukla, M. K., Leszczynski, J., Eds.; Springer: Dordrecht, Netherlands, 2008; pp 343–367.

(39) Chen, H.; Li, S. Ab Initio Study on Deactivation Pathways of Excited 9h-Guanine. *J. Chem. Phys.* **2006**, *124*, 154315.

(40) Yamazaki, S.; Domcke, W.; Sobolewski, A. L. Nonradiative Decay Mechanisms of the Biologically Relevant Tautomer of Guanine. *J. Phys. Chem. A* **2008**, *112*, 11965–11968.

(41) Alonso, J. L.; Pena, I.; Lopez, J. C.; Vaquero, V. Rotational Spectral Signatures of Four Tautomers of Guanine. *Angew. Chem., Int. Ed.* **2009**, *48*, 6141–6143.

(42) Chin, W.; Mons, M.; Dimicoli, I.; Piuze, F.; Tardivel, B.; Elhanine, M. Tautomer Contributions to the near Uv Spectrum of Guanine: Towards a Refined Picture for the Spectroscopy of Purine Molecules. *Eur. Phys. J. D* **2002**, *20*, 347–355.

(43) Lobsiger, S.; Etinski, M.; Blaser, S.; Frey, H. M.; Marian, C.; Leutwyler, S. Intersystem Crossing Rates of S1 State Keto-Amino Cytosine at Low Excess Energy. *J. Chem. Phys.* **2015**, *143*, 234301.

(44) Lobsiger, S.; Trachsel, M. A.; Frey, H. M.; Leutwyler, S. Excited-State Structure and Dynamics of Keto-Amino Cytosine: The $1\pi\pi^*$ State Is Nonplanar and Its Radiationless Decay Is Not Ultrafast. *J. Phys. Chem. B* **2013**, *117*, 6106–6115.

(45) Lobsiger, S.; Leutwyler, S. The Adiabatic Ionization Energy and Triplet T-1 Energy of Jet-Cooled Keto-Amino Cytosine. *J. Phys. Chem. Lett.* **2012**, *3*, 3576–3580.

(46) Nir, E.; Hunig, I.; Kleinermanns, K.; De Vries, M. S. The Nucleobase Cytosine and the Cytosine Dimer Investigated by Double Resonance Laser Spectroscopy and Ab Initio Calculations. *Phys. Chem. Chem. Phys.* **2003**, *5*, 4780–4785.

(47) Meijer, G.; Devries, M. S.; Hunziker, H. E.; Wendt, H. R. Laser Desorption Jet-Cooling of Organic-Molecules - Cooling Characteristics and Detection Sensitivity. *Appl. Phys. B: Lasers Opt.* **1990**, *51*, 395–403.